PHYSICAL REVIEW B VOLUME 33, NUMBER 12 15 JUNE 1986

Self-consistent electronic structures of polyacetylene

Michael Springborg
Max-Planck-Institut für Festkörperforschung, Postfach 80 06 65, D-7000 Stuttgart 80, Federal Republic of Germany

(Received 13 January 1986)

The recently developed first-principles linear-muffin-tin-orbital method for calculating the electronic structure of helical polymers is applied to polyacetylene. Total energies, charge densities, and energy bands are calculated for five different geometries of *trans*- and *cis*-polyacetylene. The dimerization of *trans*-polyacetylene is furthermore investigated and the configuration coordinate u_0 is determined. It is analyzed whether the results can be explained with simple model Hamiltonians of the Su-Schrieffer-Heeger type.

I. INTRODUCTION

The discovery[1] that polyacetylene upon doping can increase its conductivity by many orders of magnitude has led to an enormous growth in the interest in this compound and many attempts to explain this property have been undertaken.

The situation is complicated by the irregularity of polyacetylene. A typical sample consists of disordered fibers, which by stretching the sample can be made somewhat parallel. Each fiber contains many shorter and longer almost parallel macromolecules. The outcome of an experiment will accordingly be a superposition of interfiber, intrafiber, and intramacromolecular effects.

A theoretician, on the other hand, is forced to consider idealizations of this structure: isolated, finite, or infinite macromolecules, or some three-dimensional, regular structure. The most common idealization is a single, isolated, infinite polyacetylene polymer.

This polymer is made up of carbon atoms each bonded via σ bonds formed by planar sp^2 hybrids to two neighboring carbon atoms and to a single hydrogen atom. The last valence electron of carbon is in π bonds perpendicular to the plane of the three sp^2 hybrids. The polymer is accordingly considered to be planar. Depending on how the carbon-carbon bonds are oriented with respect to each other different polyacetylene geometries can be generated of which the *trans* and *cis* isomers are the ones of highest symmetry.

Su, Schrieffer, and Heeger[2] (SSH) proposed a model for explaining the conductivity properties of the *trans* isomer. Their model is based on a model Hamiltonian for the carbon backbone, which is the sum of three terms: a kinetic-energy term for nuclear motion, a tight-binding term for π-electron interactions, and a harmonic term describing the σ-electron bonding energy expanded to lowest order about the undimerized state. Excited states of the total system, the so-called solitons, are according to their model responsible for the conducting properties of *trans*-polyacetylene.

This model has been improved and investigated by many authors (for a recent review, see, e.g., Ref. 3), but it is still not clear whether the explanation offered by Su, Schrieffer, and Heeger is correct (see, e.g., Ref. 4).

Before being able to attain a deeper understanding of the excited states of a polyacetylene polymer, it is important to have a good description of the ground state, and compare it with some of the assumptions behind the SSH model Hamiltonian. Some of the questions that should be answered are the following:

Is a model treating only π electrons reasonable?

It might be expected that a quasi-one-dimensional system with one electron per CH unit will undergo a Peierls distortion, leading to alternating carbon-carbon bond lengths. Is this behavior also found for a more detailed model treating all the electrons?

How well do parameters for a model Hamiltonian extracted from detailed analysis agree with those of the SSH model Hamiltonian?

How important are longer-range interactions between the π electrons neglected in the original SSH model but to some extent included in later improvements?

Furthermore, detailed investigations should be able to compare the *trans* and *cis* isomers.

A large number of detailed calculations on ground-state properties of polyacetylene have been reported ranging from semiempirical calculations,[5-12] via Hartree-Fock calculations,[13-26] to Hartree-Fock calculations improved with inclusion of some parts of correlation effects,[27,28] and to calculations within the framework of the local-density approximation.[29-36] The interest has mostly concentrated on calculating the geometries and the one-electron energy bands. All parameter-free calculations on both *trans* and *cis* isomers were performed at the Hartree-Fock level with a minimal basis set, except for the Hartree-Fock calculations by Kirtman *et al.*[21] and by Teramae *et al.*,[23] and the density-functional calculations by Grant and Batra.[30,35] Of the exceptions, only Grant and Batra included correlation effects, but, on the other hand, they did only consider one fixed *trans* and one fixed *cis* geometry.

The aim of the present paper is to present results of self-consistent calculations on different geometries of both *trans*- and *cis*-polyacetylene. The method, recently developed,[37] is based on the local-density scheme (i.e., correlation effects are included). The linear muffin-tin orbital (LMTO) basis set used is better than minimal but not completely of double-ζ quality. Our analysis will be

©1986 The American Physical Society

separated into two parts. First, we will examine the one-electron energy bands and the electron densities for different geometries of *trans*- and *cis*-polyacetylene. Second, we will utilize energy bands and total energies from the *trans* isomer to try to answer some of the questions raised in connection with the SSH model Hamiltonian.

The outline of the paper is as follows. A very detailed description of the method applied is given in Ref. 37, so Sec. II will only contain a short introduction sufficient to clarify the terminology used later. In Sec. III we describe the geometries we have considered. Section IV contains our one-electron energy bands and electron densities for the *trans* and *cis* isomers, and, in Sec. V, these are compared with results of other calculations. The dimerization of *trans*-polyacetylene and the SSH model Hamiltonian are examined in Sec. VI, and, finally, Sec. VII contains the conclusion.

II. METHOD

Within the usual Born-Oppenheimer approximation and in the local approximation to the density-functional scheme, we seek the one-electron eigenfunctions to the effective Schrödinger equation (in Rydberg atomic units),

$$\hat{h}_{\text{eff}}\psi_i(\mathbf{r})=[-\nabla^2+v(\mathbf{r})]\psi_i(\mathbf{r})=\varepsilon_i\psi_i(\mathbf{r}) \ , \tag{1}$$

where the potential $v(\mathbf{r})$ is the sum of the Coulomb potential from the nuclei, $v_n(\mathbf{r})$, and from the electrons, $v_e(\mathbf{r})$, plus the exchange-correlation potential in the local-density approximation, $v_{\text{xc}}(\mathbf{r})$. v_e and v_{xc} depend on the electron density

$$\rho(\mathbf{r})=\sum_{\substack{i=\text{occupied}\\ \text{states}}}|\psi_i(\mathbf{r})|^2 \ . \tag{2}$$

Equations (1) and (2) are to be solved self-consistently.

The eigenfunctions $\psi_i(\mathbf{r})$ are expanded in LMTO's, which requires some description. Inside nonoverlapping atomic spheres, placed such that each nucleus occupies a center, the basis functions are described analytically as solutions to numerical, one-dimensional, effective Schrödinger equations of the form (1) obtained by considering only the spherical symmetric part of the potential inside the sphere. In the interstitial region outside all spheres the LMTO's are given analytically as spherical Hankel functions of the first kind times spherical harmonics. The functions are defined such that they are continuous and differentiable everywhere.

Inside the atomic spheres the electron density calculated from (1) and (2) can easily be expressed as a one-center expansion as

$$\rho(\mathbf{r})=\sum_{l,m}\rho_{l,m}(r)Y_{l,m}(\hat{\mathbf{r}}) \ . \tag{3}$$

In the interstitial region we approximate the calculated electron density using a least-squares fit. This step is necessary to obtain the potential generated by the interstitial density used for the total energy and for the next iteration in a self-consistent scheme.

By comparing densities for different compounds, some information on the similarities and differences between them can be obtained. The multipoles

$$q_{l,m}=\sqrt{4\pi}\int_0^s r^l\rho_{l,m}(r)dr \tag{4}$$

obtained from (3) are here particularly useful.

Our method can, in principle, be used for any system, but the present computer codes we have made are restricted to calculating the electronic distribution of the ground state of a single isolated, infinite, periodic, helical polymer. Polyacetylene is considered to have these characteristics.

The primitive symmetry operation that maps such a polymer onto itself can be described as a combined rotation, v, around the symmetry axis and a translation, h, along it. The two parameters (h,v) uniquely define the symmetry.

Two sets of coordinate systems are appropriate for such a system. First, a global right-handed one with the z axis along the symmetry axis. In this coordinate system, the ith atom in the nth unit cell is placed at

$$\begin{aligned} x&=r_i\cos(u_{n,i}) \ , \\ y&=r_i\sin(u_{n,i}) \ , \\ z&=(h/v)u_{n,i}+z_i \ , \end{aligned} \tag{5}$$

with

$$u_{n,i}=nv+\phi_i \ , \tag{6}$$

and where the parameters (r_i,ϕ_i,z_i) are unique for the ith atom. Second, local right-handed coordinate systems with the z axes parallel to the symmetry axis and the x axes pointing away from it are placed on each nucleus. Bloch functions for k in the Brillouin zone, $k\in[-\pi/v,\pi/v]$, can then be formed from the *local* basis functions.

III. GEOMETRY OF POLYACETYLENE

The high-symmetry forms of planar polyacetylene, the *trans* and *cis* isomers, may be considered in two different forms depending on whether all carbon-carbon bonds have the same length or alternating lengths (i.e., whether the polymer is dimerized). For the dimerized *cis* isomer, there are two possibilities, each differing in which carbon-carbon bonds are taken to be shorter and which longer.

In Fig. 1 we schematically depict the five different geometries using a simple bond-order picture in which the dimerized isomers have alternating single and double carbon-carbon bonds and where the nondimerized isomers have $1\frac{1}{2}$ carbon-carbon bonds. Geometries I and II correspond to the *trans* isomers and III–V to the *cis* isomers. Geometries II, IV, and V are the dimerized polymers. For all geometries, the global z axes are defined as pointing to the right. In the figure, we have furthermore shown the unit cell used and the numbering of the atoms inside it. For the undimerized *trans* isomer a unit cell with only one CH unit had been sufficient, but with two units, we obtain identical treatments of all geometries.

The parameter v describing the helical symmetry is for the *trans* isomers with translational symmetry $v=2\pi$, and for the *cis* isomers with zig-zag symmetry $v=\pi$. The rest of the parameters describing the geometries is to be found from the bond lengths and bond angles.

From x-ray diffraction analysis combined with crystal-packing analysis, Baughman *et al.*[38] have obtained the

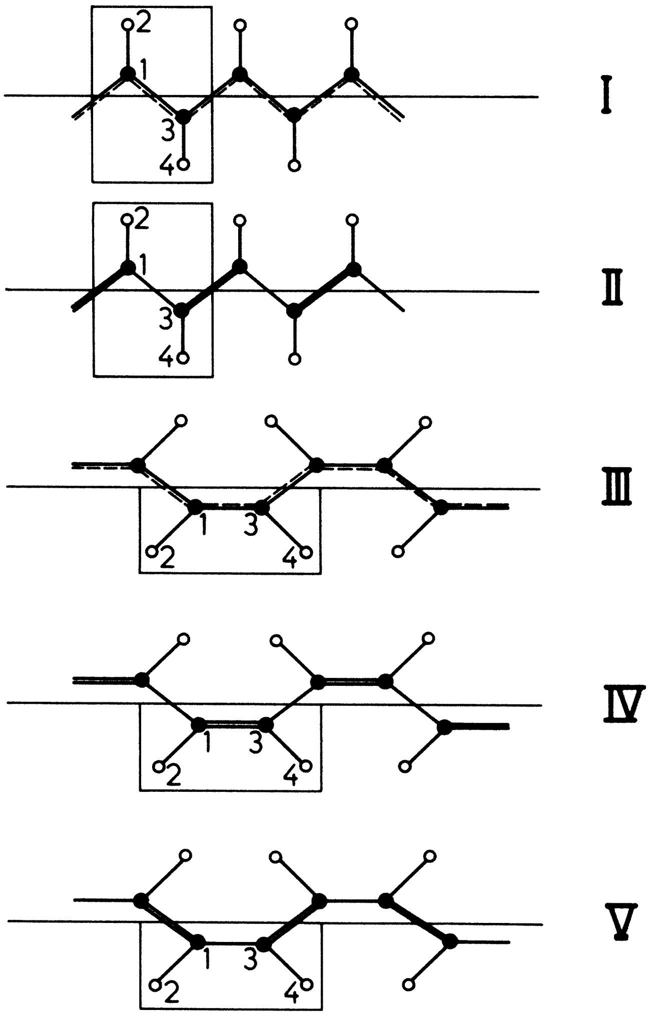

FIG. 1. Schematic representation of *trans*- (geometries I and II) and *cis*- (geometries III–V) polyacetylene. Carbon (hydrogen) atoms are symbolized with solid (open) circles. The single, double, and $1\frac{1}{2}$ bonds are represented with —, =, and $\overset{-}{=}$, respectively. Also drawn are the unit cells used in the calculations. The numbering of the atoms inside the unit cell is indicated. Finally, the helical symmetry axes are shown. The positive direction is assumed to be towards the right.

geometries of the two alternating *cis* isomers. The carbon-carbon bond lengths were found to be 1.35 and 1.46 Å, and the angles deviated only little from 120°. The carbon-hydrogen bond length was 1.09 Å. For the dimerized *cis* isomers, we will use those values, and for the dimerized *trans* isomers we will use the same bond lengths but set all angles identical and equal to 120°. Also, for the nondimerized polymers (geometries I and III) the angles are set to 120°. The hydrogen-carbon bond length is kept at 1.09 Å, whereas the carbon-carbon bond length is chosen as the optimized value on the *cis* nonalternating isomer by Yamabe *et al.*,[7] i.e., 1.39 Å. In agreement with the semiempirical results of Pauling,[39] this value is smaller than the average of the values for the alternating bond lengths.

With those values of the bond lengths and angles, we can determine the parameters (r_i,ϕ_i,z_i) and (h,v) for the five geometries of Fig. 1. The results are displayed in Table I in atomic units.

In studying the dimerization of *trans*-polyacetylene we use the following one-parameter approach. In the simplest bond picture one of the four valence electrons of the carbon atom will in a sp^2 hybrid participate in a σ bond with the hydrogen 1s electron. The other three valence electrons will be involved in bonds with the two nearest carbon neighbors. Hence, the sum of the bond orders of the two carbon-carbon bonds per carbon atom will be 3. By choosing the bond orders to be $1+x$ and $2-x$, we can use the bond lengths given by Pauling,[39]

$$\begin{aligned} D_{1+x} &= \left[1.504-0.170\times\frac{1.84x}{1+0.84x} \right] \text{Å} , \\ D_{2-x} &= \left[1.504-0.170\times\frac{1.84(1-x)}{1.84-0.84x} \right] \text{Å} . \end{aligned} \qquad (7)$$

The hydrogen-carbon bond length is kept fixed at 1.09 Å and all bond angles are set to 120°. Su, Schrieffer, and Heeger[2] followed a different path. They chose the length of the unit cell and the distance between the helical axis and the carbon atoms to be constant. Furthermore, effects of the positions of the hydrogen atoms were neglected. We believe, however, that had we chosen the path of SSH our conclusions would have been unaltered.

Finally, it can be mentioned that the bond lengths 1.35 and 1.46 Å used in the comparison between *trans*- and *cis*-polyacetylene correspond to $x=0.16$ (± 0.0005).

IV. RESULTS

Strictly speaking, the energy bands calculated within the density-functional scheme are not to be identified with excitation energies, except for the highest occupied level which corresponds to the ionization potential.[40] However, experience has shown that interpreting the energy bands as one-electron excitation energies is a good approximation and it will therefore also be done here.

In Fig. 2 we show the self-consistent one-electron energy bands for the five geometries of Fig. 1 and Table I.

As is to be expected, the *trans* and *cis* isomers show both similarities and differences. For all geometries the valence bands consist of four bands of σ symmetry (i.e., the eigenstates are even with respect to the polymer plane) and one band of π symmetry (odd). The states closest to the Fermi level (ε_F) are for all geometries of π symmetry. The π_1 bands have for the *trans* geometries their maxima at $k=\pi/v$, whereas for the *cis* geometries the maxima occur at $k=0$. The situation is reversed for the π_2 bands. This difference between the *trans* and *cis* isomers is solely caused by our definitions: For the zig-zag symmetry (the *cis* isomers, $v=\pi$) the local p_y orbitals are antiparallel in neighboring unit cells, whereas for the translational symmetry (the *trans* isomers, $v=2\pi$) they are parallel.

All isomers have σ_1 bands of mainly carbon s and p nature. The other three σ valence bands are more complicated and are of carbon s and p and hydrogen s and p na-

TABLE I. Geometries used for the five different types of polyacetylene. For further explanation see text.

	Geometry				
	I	II	III	IV	V
h	4.550	4.600	3.940	4.223	4.222
v	2π	2π	π	π	π
r_1	0.658	0.663	1.138	1.097	1.045
ϕ_1	0	0	0	0	0
z_1	0	0	0	0	0
r_2	2.717	2.722	2.922	2.881	2.829
ϕ_2	0	0	0	0	0
z_2	0	−0.047	−1.030	−1.030	−1.030
r_3	0.658	0.663	1.138	1.097	1.045
ϕ_3	π	π	0	0	0
z_3	0	0.120	2.627	2.551	2.759
r_4	2.717	2.722	2.922	2.881	2.829
ϕ_4	π	π	0	0	0
z_4	0	0.167	3.657	3.581	3.789

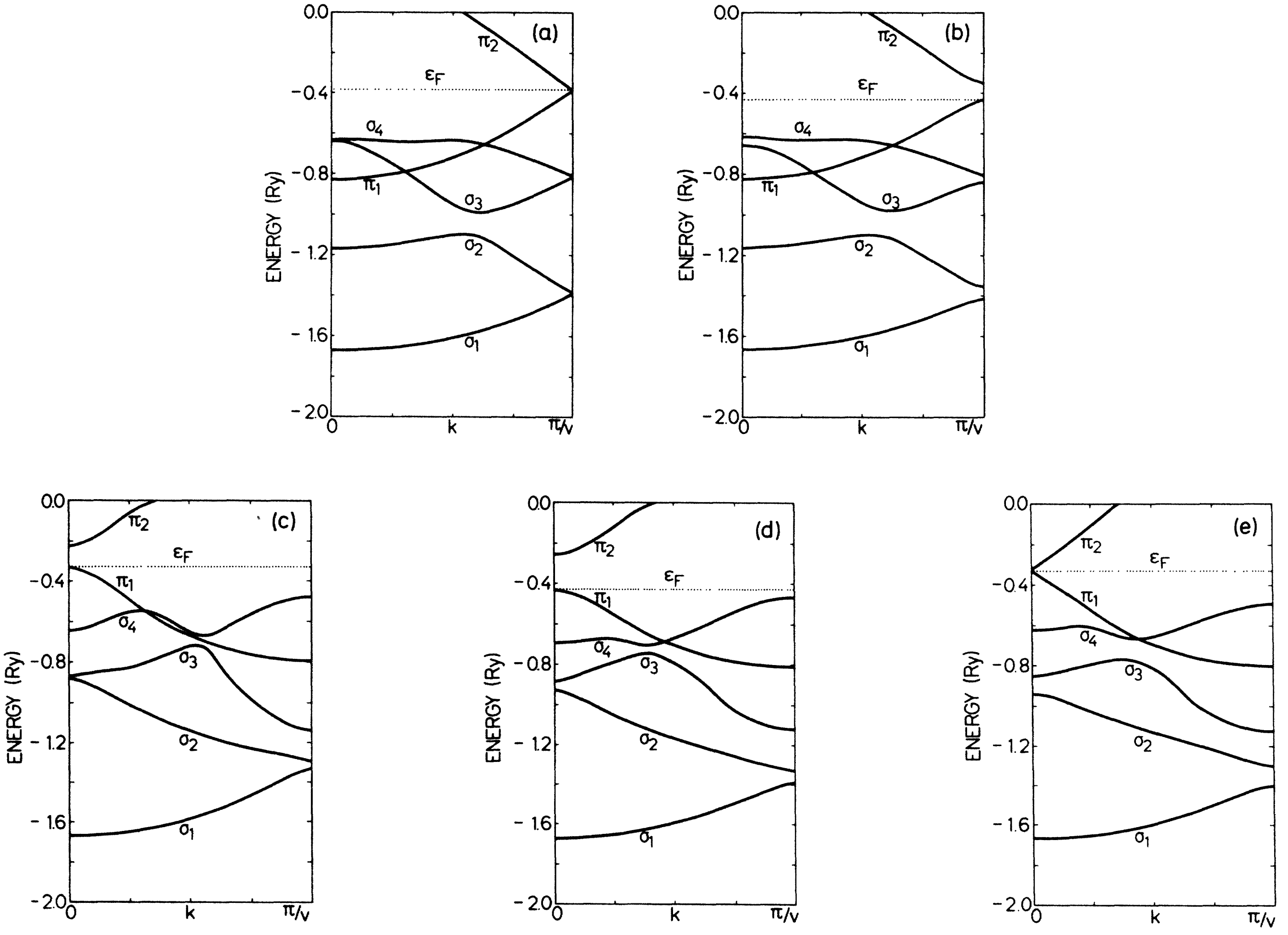

FIG. 2. Self-consistent one-electron energy bands for the five symmetries of Fig. 1 and Table I. Panels (a)—(e) correspond to the geometries I—V, respectively.

ture. For the *trans* isomers, the σ_2 and σ_3 bands show an avoided crossing, as the σ_3 and σ_4 bands do for the *cis* isomers. We suggest this difference be used in distinguishing between *trans*- and *cis*-polyacetylene. For example, x-ray photoelectron spectroscopy measuring essentially the density of occupied states should give different spectra for the *trans* and *cis* isomers. We have not been able to find experimental verification of this prediction: The *cis*-rich films tend to change into *trans*-rich films at normal experimental conditions,[41] which explains why we only have been able to find spectra for the *trans* isomer.

For undimerized *trans*-polyacetylene (geometry I) a unit cell with one CH unit had been sufficient. Therefore, the bands in Fig. 2 for this geometry are all doubly degenerate at $k=\pi/v$. When dimerizing (passing to geometry II), the bands will essentially remain unchanged, except near $k=\pi/v$ where gaps will show up. In contrast to this, undimerized *cis*-polyacetylene (geometry III) does not have such a higher symmetry, which causes degeneracies.

The decrease of the direct π_1-π_2 gap at $k=0$ for the *cis* isomers when passing from geometry IV via III to V can be explained as being partly due to long-range effects. A simple tight-binding Hamiltonian only treating the carbon p_y electrons will illustrate this. Using the numbering of Fig. 1 for the atoms and letting (n,i) denote a local carbon p_y orbital on atom i in unit cell n, we will introduce the following hopping integrals (see Fig. 3):

$$\begin{aligned}
&\langle (0,1)\,|\,\hat{h}\,|\,(0,3)\rangle=\beta_1\ ,\\
&\langle (0,1)\,|\,\hat{h}\,|\,(-1,3)\rangle=-\beta_2\ ,\\
&\langle (0,1)\,|\,\hat{h}\,|\,(-1,1)\rangle=-\beta_3\ ,\\
&\langle (0,1)\,|\,\hat{h}\,|\,(-2,3)\rangle=\beta_4\ ,
\end{aligned}\tag{8}$$

plus the analogues.

The k-dependent 2×2 Hamiltonian matrix is then

$$\begin{aligned}
&H_{11}(k)=H_{22}(k)=-2\beta_3\cos(kv)\ ,\\
&H_{12}(k)=H_{21}^{*}(k)=\beta_1-\beta_2e^{ikv}+\beta_4e^{2ikv}\ ,
\end{aligned}\tag{9}$$

giving a direct gap at $k=0$ of

$$2\,|\beta_1-\beta_2+\beta_4|\ . \tag{10}$$

Since $\beta_i>0$ decreases with increasing interatomic distance, we have

$$\begin{aligned}
&\beta_1(\mathrm{III})=\beta_2(\mathrm{III})\ ,\\
&\beta_1(\mathrm{IV})>\beta_2(\mathrm{IV})\ ,\\
&\beta_1(\mathrm{IV})=\beta_2(\mathrm{V})\ ,\\
&\beta_1(\mathrm{V})=\beta_2(\mathrm{IV})\ ,\\
&\beta_1(\mathrm{IV})>\beta_1(\mathrm{III})\ ,\\
&\beta_4(\mathrm{IV})>\beta_4(\mathrm{III})>\beta_4(\mathrm{V})\ .
\end{aligned}\tag{11}$$

This explains the observed behavior. The long-range β_4 cannot be neglected. If done, geometry III would have corresponded to a zero-gap semimetal and the gaps of geometries IV and V would have been identical. We will come back to the long-range hopping integrals in Sec. VI.

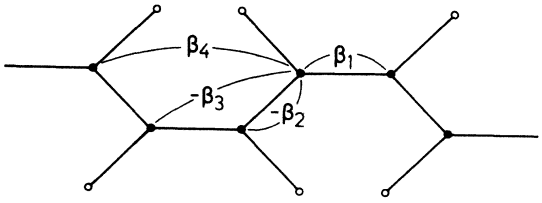

FIG. 3. Schematic representation of the π-electron hopping integrals used for the *cis* isomers.

In Table II we have collected some of our calculated bandwidths and band gaps. The comparison with the results from other calculations is left for the next section. We see in the table that especially the band gap depends on the geometry. This value should therefore be taken with some caution, keeping in mind that our geometries have not been optimized.

Geometry III, which has the smallest unit cell, has, to some extent, larger bandwidths than the other *cis* isomers. Especially the σ_1 bands corresponding to carbon-carbon bonds are accordingly expected to show this tendency. Similarly, the more-closely-packed *cis*-polyacetylene has, in general, broader bands than *trans*-polyacetylene.

The relative total energies given in Table III show that we find the commonly established picture that dimerized *trans*-polyacetylene is the most stable isomer, but it should be kept in mind that we have not optimized the geometries. We believe that an optimization will especially affect the more-closely-packed *cis* structures. As demonstrated for the gap in the *cis* isomers, the one-electron eigenvalues for these depend somewhat on second- and third-nearest-neighbor interactions. For the *trans* isomers, these neighbors are farther apart and should accordingly be less important. Also, the convergence of the lattice summations is expected to be more important for the more-closely-packed *cis* isomers than for the more open *trans* isomers. Our total energies in Table III show the largest fluctuations for the *cis* isomers that might be interpreted in this way.

That the *cis* isomers are more closely packed than the *trans* isomers can be seen in Fig. 3, where we show for the five geometries the approximate electron density $\tilde{\rho}(\mathbf{r})$ described in Sec. II. Strictly speaking, $\tilde{\rho}(\mathbf{r})$ is only valid in the interstitial region, but in Fig. 4 we have continued it into the outer parts of the atomic spheres. Geometries II, IV, and V clearly show the dimerization when compared with geometries I and III. Although the hydrogen atoms become much closer in the *cis* polymers than in the *trans* polymers, it is seen that there is only little interaction between them.

The electron densities are seen to be well localized within the polymer, justifying treating only a single, isolated macromolecule.

Inside the spheres we expand the electron density according to (3). Since the results depend only slightly on geometry, we have chosen to present only one set of figures, namely those for geometry III. The s, p_x, and p_z components of the electron density inside the atomic

TABLE II. Bandwidths, fundamental band gap, and ionization potential in eV as obtained by different theoretical methods. The calculations of Refs. 5–12 are semiempirical, of Refs. 13–26 of Hartree-Fock type, of Refs. 27 and 28 of Hartree-Fock type with inclusion of some correlation effects, and the rest of local-density type. The values marked with an asterisk correspond to optimized geometries. For more details, see text.

			Geometry			
	I	II	III	IV	V	References
σ_1 bandwidth				11.54,11.48		9
		5.01				15*
		6.78				18
	3.88	3.39	4.64	3.87	3.63	This work
σ_2 bandwidth				6.50		9
	3.95	3.46	5.66	5.58	4.99	This work
σ_3 bandwidth				13.85,16.50		9
	4.83	4.44	5.76	5.19	4.87	This work
σ_4 bandwidth				6.57,6.27		9
		3.16,3.46				15*
		4.00				18
	2.47	2.54	2.73	3.42	2.42	This work
π_1 bandwidth				10.24,10.32		9
		5.0				11
		7.95,7.76				15*
		6.50		6.42	6.53	18
		6.23		6.45	6.34	21*
	6.02	5.31	6.31	5.18	6.39	This work
Total valence-band width		25.36,24.68				15*
		25.66				18
		19.2				34
		21.08				35
	17.49	16.74	18.23	16.91	18.15	This work

spheres around carbon atom 1 (see Fig. 1) and hydrogen atom 2 are—multiplied by r^2—depicted in Fig. 5. The sphere radii were 1.274 a.u. for the carbon atom and 0.784 a.u. for the hydrogen atom.

The s component for the carbon atom clearly shows the $1s$ core electrons and the valence electrons in the outer region. The p_x component describes the difference in the strength of the bonds to the nearest hydrogen atom and to the nearest carbon atom of the neighboring unit cell. The p_z component can similarly be interpreted as comparing the strength of the bond to the nearest carbon atom in the same unit cell with the strength of the bonds to the two above-mentioned atoms.

The p components for the hydrogen atom almost solely describe the bonds to the nearest carbon atom.

For the *trans* isomers, the p components of the carbon atom need to be interpreted slightly differently. The p_z component mainly describes the dimerization, whereas the p_x component compares the strength of the bond to the hydrogen atom with that of the bonds to the two nearest carbon atoms.

It should be noticed that for an isolated atom the total electron density from the three ideal sp^2 hybrids will give rise to no p components in the plane of the hybrids.

In comparing the different geometries, we will use the multipoles defined in Eq. (4). They are tabulated in Table IV.

The s components and the hydrogen p components differ only slightly for the five geometries. The largest differences are found for the carbon p components. These differences are easily understood with the just-described interpretation and Fig. 1 in mind.

V. COMPARISON WITH OTHER CALCULATIONS

Before comparing with the other calculations for polyacetylene, we will briefly describe the methods applied.

Whangbo *et al.*[5] reported extended Hückel calculations on all the geometries of Fig. 1, except geometry III. Yamabe *et al.*[6,7] used the semiempirical CNDO/2 (where CNDO denotes complete neglect of differential overlap) method on optimized geometries for all five structures of Fig. 1. With this approach, they calculated energy bands and total energies.

Young *et al.*[8] reported semiempirically calculated band structures for two different geometries of alternating *trans*-polyacetylene within the EHCO and MNDO methods (EHCO, extended Hückel crystal orbital; MNDO, modified neglect of differential overlap). In Ref. 9 Young demonstrates the simplifications obtained when using the helical symmetry for the *cis* isomer. He presents results calculated both for the translational and for the helical symmetry for *cis*-polyacetylene within the EHCO method.

TABLE II. (*Continued*).

	Geometry					
	I	II	III	IV	V	References
Smallest	0	0.96		1.23	0.71	5
π_1-π_2	0	7.46	5.75	8.43		6*
band gap		0.8,3.5				8
				3.79		9
		4.9				11
	0	7.24	8.74	3.95	10.39	13
		8.05				15*
	0	9.74	5.21	8.19	7.83	16
		1.4		1.5	1.3	20
		11.64		11.70	11.62	21*
	0	8.71	4.63	8.98	8.98	22*
	0	4.43				25*
		6.88				26*
		2.98				28*
	0					29
		0.8		1.2		30
		1.6		1.7	1.2	31
		0.6				32*
		0.6				33*
		1.6				34
		1.3				36
	0	1.10	1.34	2.31	0.09	This work
Ionization	4.09	7.82	5.75	2.52		7*
potential		7.8				11
		7.13				14*
		5.31				15*
	0.21	5.27	2.81	4.56	4.54	16
		6.61				18
		4.7		4.8	4.7	20
		6.19		6.24	6.21	21*
		4.98				28*
	11.56					29
	5.22	5.87	4.45	5.84	4.53	This work

The helical symmetry was also used by Elert and White,[10] who optimized the geometry for the *cis* isomer within the MNDO method. They find a nonplanar geometry with energy only slightly above the planar ground state. A spectroscopically parametrized CNDO method has been applied on dimerized *trans*-polyacetylene by Ford *et al.*[11] Al-Jishi *et al.*[12] report tight-binding bands for the alternating *trans* isomer. In contrast to most other works, they find π bands well separated from the valence σ bands.

Some of the first Hartree-Fock calculations on polyacetylene were reported by Kertész *et al.*[13] for all five geometries of Fig. 1 for fixed (i.e., unoptimized) bond lengths and angles. Their calculations were performed with the minimal STO-3G (Slater-type orbital described by three Gaussians) basis set. From calculations on finite molecules, they demonstrated that such a basis is far from being converged.

Karpfen and Petkov[14,15] optimized the geometry for the alternating *trans* isomer using the Hartree-Fock method with a minimal STO-3G basis[14] and with a minimal STO-3G basis set as well as the better $8s4p/4s$ basis.[15] The improved basis set lowers the total energy per C_2H_2 unit by approximate 25 eV. They reported the band structures for the optimized geometries.

Suhai[16] performed Hartree-Fock calculations on exactly the same structures as we have. He used a minimal STO-3G basis and investigated cutoff errors introduced by unconverged lattice summations.

Karpfen and Höller[17] optimized the five geometries with a minimal STO-3G basis set within the Hartree-Fock approximation. Brédas *et al.*[18,19] used a valence effective Hamiltonian (VEH) technique in which model Hartree-Fock calculations on smaller molecules with double-ζ basis sets define effective Hamiltonians for the polymers. They calculated the energy bands for all the alternating structures (geometries II, IV, and V).

From Hartree-Fock calculations with both the minimal STO-3G and the better 3-21G basis set on finite molecules, Kirtman *et al.*[21] made extrapolations to the polymers. The geometries were optimized. Results were reported for all the alternating structures.

TABLE III. Relative total energies in eV per C_2H_2 unit found by different approaches for the structures I—V of Fig. 1. Only the values for references marked with an asterisk correspond to optimized geometries. The calculations of Refs. 5—12 are semiempirical. For the Hartree-Fock calculations (Refs. 13—26) and the Hartree-Fock calculations with inclusion of some correlation effects (Refs. 27 and 28), the total energy in Ry per C_2H_2 unit has been included in parentheses for a single geometry. These values can be compared with the free-atom values of -1 Ry for hydrogen and -75.679 Ry for carbon [F. Sasaki and M. Yoshimine, Phys. Rev. A 9, 17 (1974)], giving -153.358 Ry per C_2H_2 unit. For the density-functional calculations (Refs. 29—36 and present work), the binding energies in eV per C_2H_2 are given for a single geometry. Mintmire and White (Refs. 32 and 33) use atomic energies calculated with the same basis set as used in the polymer calculations and neglect spin-polarization energies, thereby overestimating the atomic energies. Our atomic energies have been calculated from numerical solutions to the effective Schrödinger equation with addition of the spin-polarization energy.

			Geometry		
References	I	II	III	IV	V
5	0.08	0		0.47	0.42
6	0.16	0	0.24	0.07	
7			0.21	0	0.10
13	0.29	0 (−151.903)	−1.38	−0.68	−1.72
15*	0.07	0 (−153.728)			
16	−0.63	0 (−153.737)	−0.70	−1.11	−1.00
17*	0.31	0 (−151.896)	0.23	0.08	0.09
21*		0 (−151.896)		0.09	0.09
22*	0.38	0 (−151.892)	0.36	0.08	0.09
27*,28*	0.09	0 (−154.336)			
32*,33*	0.03	0 (18.55)			
This work	0.10	0 (11.15)	0.84	1.65	0.60

Also, Dovesi[22] carried through Hartree-Fock calculations with a minimal STO-3G basis set. He was mainly interested in convergence properties of the calculations, and reported total energies for optimized geometries for all structures in Fig. 1.

Teramae *et al.*[23] calculated vibrational structures of all the alternating structures of polyacetylene. They used the Hartree-Fock method with both STO-3G and 4-31G basis sets. They reported optimized geometries.

Rao *et al.*[24,25] were interested in the possibility of helical nonplanar forms of polyacetylene. With both the minimal STO-3G basis set and the improved 4-31G basis set, and with the Hartree-Fock method they found evidence of nonplanar structures of the alternating isomers which were low lying in energy.

The last Hartree-Fock calculations we will consider were made by I'Haya *et al.*[26] for the alternating *trans* isomer. They examined the role of the quality of the basis set. Furthermore, they also carried out calculations using the model-potential method[42] where only valence electrons are treated. For a geometry optimized with a STO-3G basis they performed calculations with basis sets ranging from STO-3G to double-ζ $10s\,5p$ types. As found by Karpfen and Petkov, the calculated binding energy can—with improved basis sets—be increased by as much as 25 eV per C_2H_2 unit.

Suhai[27,28] included part of the correlation effects using a method based on Hartree-Fock calculations and second-order Møller-Plesset (MP) perturbation theory.[43] For both structures of the *trans* isomer, Suhai optimized the geometries with different basis sets with and without inclusion of the MP perturbation. The correlation energy he found gives a reduction of approximately 5 eV in the total energy per C_2H_2 unit.

To the author's knowledge, the first local-density calculations on polyacetylene were performed by Falk and Fleming[29] on the undimerized *trans* isomer. They used a crude muffin-tin approximation in which the potential was assumed to be spherical symmetric inside the atomic spheres and constant in the remainder of space. This explains[44] why for the *trans* isomer they obtained energy bands quite different from results of other parameter-free calculations; one has to conclude that this approximation is not justified.

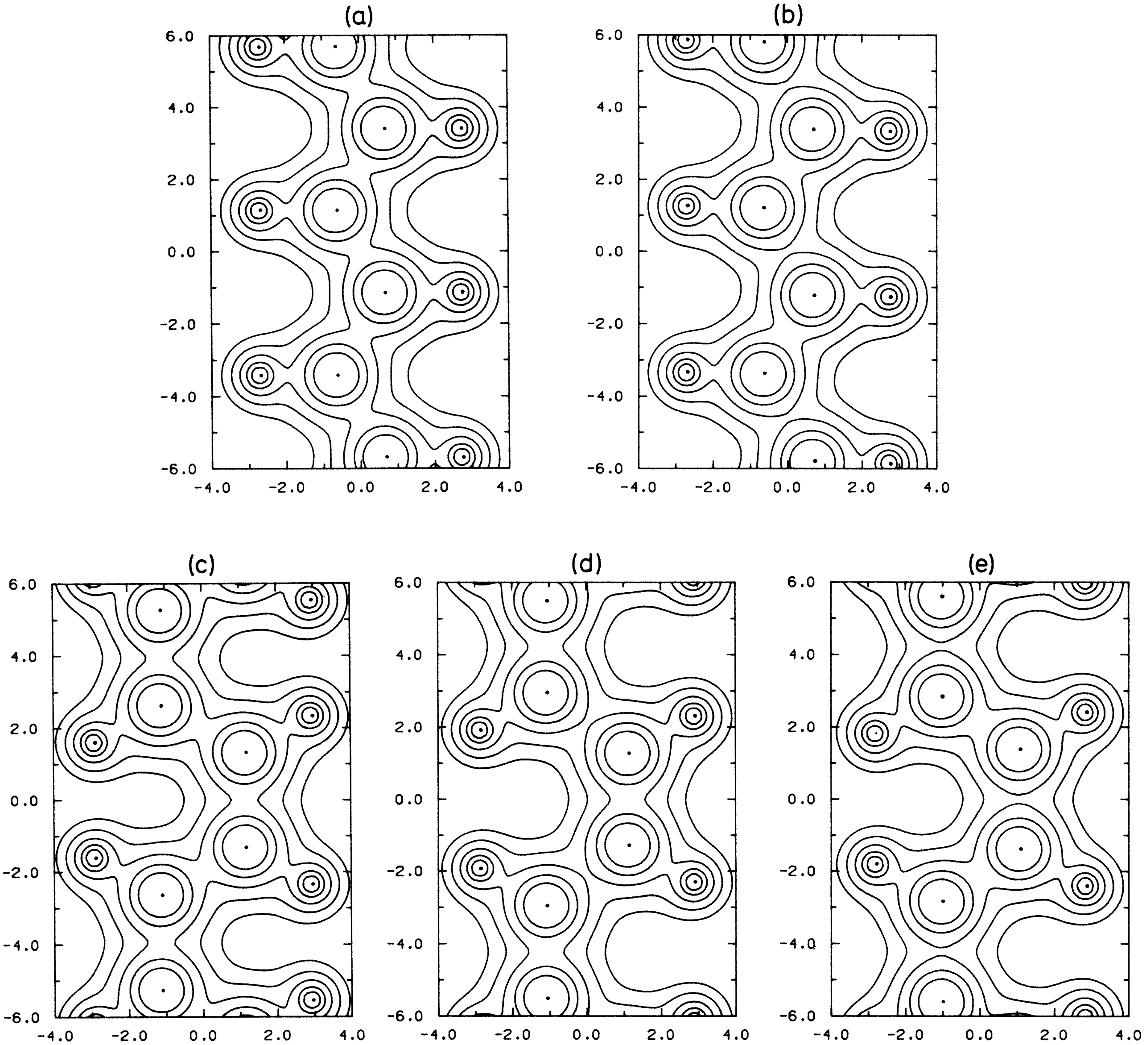

FIG. 4. Contour curves for the approximate electron density $\tilde{\rho}(\mathbf{r})$ for the five geometries of Fig. 1. Contour values are 0.8, 0.4, 0.2, 0.1, and 0.05 a.u. The densities are shown in the planes containing the nuclei. Panels (a)—(e) correspond to the geometries I—V, respectively.

Some of the only calculations on three-dimensional crystalline polyacetylene have been carried through by Grant and Batra[30,35] on the crystal structures for geometry IV of Fig. 1 proposed by Baughman *et al.*[38] (Ref. 30) and for geometry II on the structure proposed by Fincher *et al.*[45] (Ref. 35). The calculated energy bands show only slight dispersion along directions perpendicular to the chains, as should be expected. Furthermore, in Ref. 30 Grant and Batra report semiempirically obtained bands for single *trans* isomer chains. For the calculations on the three-dimensional structures, in Ref. 30 they used a non-self-consistent, first-principles, LCAO method, and in Ref. 35 the self-consistent pseudopotential method.

Kasowski *et al.*[31] also considered three-dimensional polyacetylene, but reported mainly the one-dimensional behavior. Their method has similarities with ours, but they used a minimal basis set. It is not clear how important this approximation is when considering three-dimensional structures. For one-dimensional structures, we have found that the changes arising from passing from minimal to extended basis sets are certainly not negligible. Kasowski *et al.* reported energy bands and charge densities for the highest occupied state for the alternating structures.

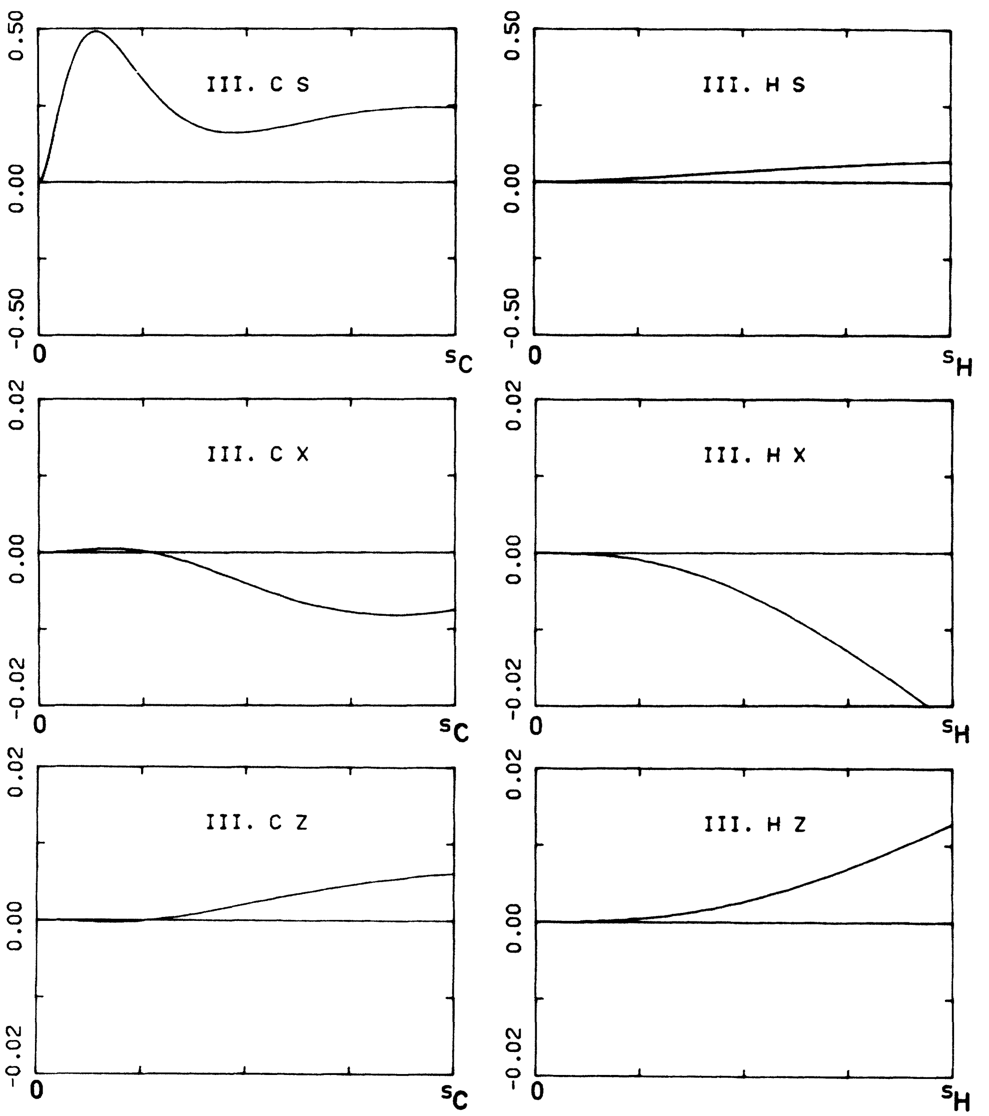

FIG. 5. Different angular components of total electron densities inside the atomic spheres multiplied by r^2 for geometry III. Carbon atom 1 (labeled C in the figure) and hydrogen atom 2 (labeled H) of Fig. 1 were considered. s, x, and z denote the s, p_x, and p_z components, respectively. ($s_C = 1.274$ a.u., $s_H = 0.784$.) Note the different scales on the y axis for the s and p components.

Mintmire and White[32,33] used a self-consistent LCAO method on *trans*-polyacetylene with the $X\alpha$ approximation for exchange and correlation effects. The geometries were partly optimized.

A similar method, but employing the local-density approximation instead of the $X\alpha$ approximation, was used by von Boehm *et al.*[34,36] non-self-consistently[34] and self-consistently,[36] but without geometry optimization and only for the dimerized isomer.

In Table III we have collected relative total energies as reported by different authors. Of the results only those of Refs. 17, 21, 22, and 27 are first-principles results on optimized geometries. Among those there seems to be agreement that the dimerized *trans* isomer is the most stable isomer. This trend is not found in all the calculations for nonoptimized geometries. However, as is seen, there is general agreement that the energy differences for the different geometries are small. Finally, we would like to point out that our calculations show polyacetylene to be stable. Our binding energy is approximately 11 eV per C_2H_2 unit upon comparison to decomposition into neutral, isolated atoms. The atomic energies are calculated numerically within the local-density scheme with the addition of the spin-polarization energy.

Table II shows some well-known trends for the bandwidths, band gaps, and ionization potentials: Hartree-Fock calculations tend to overestimate widths and gaps, whereas local-density calculations underestimate the gaps. The semiempirical methods depend crucially on the quality of the parametrizations and give varying results. With

TABLE IV. Multipoles of the electron density inside the atomic spheres for carbon (atom 1 in Fig. 1—here denoted C) and hydrogen (atom 2 in Fig. 1—here denoted H). s, x, and z are the s, p_x, and p_z components, respectively. The radii of the atomic spheres are 1.274 a.u. for carbon and 0.784 a.u. for hydrogen.

		Geometry				
		I	II	III	IV	V
C	s	3.99	3.98	3.99	3.96	3.92
C	x	−0.06	−0.05	−0.07	−0.01	−0.09
C	z	0	−0.07	0.03	0.07	−0.05
H	s	0.33	0.33	0.34	0.33	0.33
H	x	−0.05	−0.05	−0.04	−0.04	−0.04
H	z	0	0.00	0.02	0.03	0.03

this in mind, our bandwidths seem to be in good agreement with others. As mentioned in the preceding section, the band gaps of the *cis* isomers depend not only on the positions of the nearest neighbors but also on those of the second- and third-nearest neighbors. For the *trans* isomers, the band gap is expected to be mainly determined by the nearest-neighbor positions and therefore do not vary so strongly with geometry as for *cis* polyacetylene. The experimental value of the gap is 1.4—1.8 eV for *trans*-polyacetylene and slightly larger for *cis*-polyacetylene.[45,46]

The calculated ionization potentials given in Table II show when compared with the experimental values for *trans*-polyacetylene, 4.6—4.7 eV (reported in Refs. 20 and 28), that our calculations are fairly trustworthy. The perfect agreement obtained by Brédas *et al.*[20] is found by more or less arbitrary adjusting by 1.9 eV due to "polarization energy and possible shortcomings of the model."

VI. DIMERIZATION OF *TRANS*-POLYACETYLENE

As described in the Introduction, the model Hamiltonian by Su, Schrieffer, and Heeger[2,47] (SSH) is widely used for describing the excited states of *trans*-polyacetylene. However, since the model Hamiltonian can also be used for the ground state, a comparison with parameter-free calculations can throw some light on the approximations and the parameters in the SSH Hamiltonian.

Su, Schrieffer, and Heeger assume that the only allowed distortions of the perfect, undimerized polymer are those in which the nth carbon atom with its hydrogen atom move rigidly together parallel to the polymer axis by an amount u_n. Furthermore, they assume that in the perfect, dimerized polymer we have

$$u_n=(-1)^n u_0 \ . \tag{12}$$

Simple geometry gives that u_0 then is related to D_{1+x} and D_{2-x} of (7) through

$$D_{1+x}-D_{2-x}\simeq 4\cos(30^\circ)u_0=2\sqrt{3}u_0 \tag{13}$$

when neglecting the fact that (12) is not exactly fulfilled in our analysis: the length of the unit cell, h, increases from 2.414 Å for $x=0.5$ to 2.459 Å for $x=0.0$ (cf. Table V, where most of the key quantities for the calculations for the examination of the dimerization are collected). That the carbon atoms move parallel to the helical axis is better fulfilled: The distance between the carbon atoms and the axis, r_1, is found to change from 0.349 to 0.353 Å (cf. Table V).

Neglecting the kinetic energy of the nuclei, the original SSH Hamiltonian consists of two terms:

$$H=H_\sigma+H_\pi \ . \tag{14}$$

Assuming rigid σ bonds between adjacent carbon atoms and only small u_n's, the energy contribution from the σ bonds is expanded to second order in u_n as

$$H_\sigma=\tfrac{1}{2}\sum_n K(u_{n+1}-u_n)^2 \ . \tag{15}$$

A tight-binding Hamiltonian with only nearest-neighbor interactions is assumed for the π-electron contribution to the total energy,

$$H_\pi=-\sum_{n,s} t_{n,n+1}(c^\dagger_{n+1,s}c_{n,s}+c^\dagger_{n,s}c_{n+1,s}) \ , \tag{16}$$

with $c^\dagger_{n,s}$ ($c_{n,s}$) being the creation (annihilation) operator for a π electron on site n with spin s $(=\pm\frac{1}{2})$.

A further simplification was introduced by Su, Schrieffer, and Heeger: The hopping integrals $t_{n,n+1}$ were linearized around the value for the undimerized polymer,

$$t_{n,n+1}=t_0-\alpha(u_{n+1}-u_n) \ . \tag{17}$$

The π_1 bands of geometries I and II treated in the preceding sections can give us information on the π-electron Hamiltonian H_π. A generalization of (16),

$$H_\pi=-\sum_{n,s}\sum_{m=1}^{2} t_{n,n+m}(c^\dagger_{n+m,s}c_{n,s}+c^\dagger_{n,s}c_{n+m,s}) \ , \tag{18}$$

where also second-nearest-neighbor interactions are included, will give an occupied π_1 band of the form

$$\varepsilon(k)=2t_{0,2}\cos(kv)-[t_{0,1}^2+t_{0,-1}^2+2t_{0,1}t_{0,-1}\cos(kv)]^{1/2} \ , \tag{19}$$

except for a constant. With a least-squares fit to the π_1 bands at geometries I and II in Fig. 2, we can determine

TABLE V. Key quantities in the examination of the dimerization of *trans*-polyacetylene. x defines the carbon-carbon bond orders, D_{1-x} and D_{2-x} the lengths. h is the length of the unit cell, r_1 the distance from the helical axis to the carbon atoms. u_0 describes the dimerization, E_{tot} is the relative (Rel.) total energy per C_2H_2 unit. Furthermore, the values of the five valence bands are given at the zone center and the zone edge. The two values of the energy gap E_G are the values from the first-principles calculations (first value) and that from the tight-binding Hamiltonian (second value). $q_{C,s}$, $q_{C,x}$, and $q_{C,z}$ give the s, p_x, and p_z multipoles at the electron distribution inside the carbon sphere (radius 1.260 a.u.) of atom 1, geometry II in Fig. 1.

	x					
	0.00	0.10	0.20	0.30	0.40	0.50
D_{1+x} (Å)	1.504	1.475	1.450	1.429	1.410	1.394
D_{2-x} (Å)	1.334	1.344	1.355	1.367	1.380	1.394
h (Å)	2.459	2.442	2.430	2.421	2.417	2.414
r_1 (Å)	0.353	0.351	0.350	0.349	0.349	0.349
u_0 (Å)	0.049	0.038	0.027	0.018	0.009	0.000
Rel. E_{tot} (eV)	0.286	0.093	0.005	0.042	0.156	0.242
$\sigma_1(0)$ (eV)	−22.45	−22.52	−22.61	−22.65	−22.67	−22.67
$\sigma_1(\pi/v)$ (eV)	−19.74	−19.65	−19.57	−19.43	−19.31	−19.18
$\sigma_2(0)$ (eV)	−15.73	−15.80	−15.83	−15.85	−15.86	−15.86
$\sigma_2(\pi/v)$ (eV)	−18.20	−18.44	−18.71	−18.85	−19.01	−19.08
$\sigma_3(0)$ (eV)	−9.23	−9.20	−9.20	−9.11	−9.02	−8.97
$\sigma_3(\pi/v)$ (eV)	−11.35	−11.29	−11.26	−11.18	−11.13	−11.07
$\sigma_4(0)$ (eV)	−8.03	−8.20	−8.34	−8.38	−8.44	−8.48
$\sigma_4(\pi/v)$ (eV)	−10.67	−10.80	−10.89	−10.95	−11.04	−11.06
$\pi_1(0)$ (eV)	−11.05	−11.11	−11.20	−11.22	−11.25	−11.24
$\pi_1(\pi/v)$ (eV)	−6.24	−6.13	−5.91	−5.76	−5.50	−5.41
E_G (eV)	1.71	1.37	0.97	0.64	0.31	0.01
E_G (eV)	1.86	1.50	1.12	0.74	0.37	0.00
$q_{C,s}$	3.92	3.93	3.93	3.93	3.94	3.94
$q_{C,x}$	−0.04	−0.05	−0.05	−0.05	−0.05	−0.05
$q_{C,z}$	−0.10	−0.08	−0.06	−0.05	−0.03	0.00

the hopping integrals as a function of interatomic distance D. We obtain

D (Å)	t (eV)
1.35	4.06
1.39	3.78
1.46	3.42
2.41	0.38
2.43	0.38

(20)

Since it is well known that the local-density approximation for exchange and correlation effects might produce considerable errors in conduction energy levels, we have chosen to consider only the occupied states in obtaining the parameters in (20).

Equation (19) will predict the following valence- (ε_{VB}) and conduction- (ε_{CB}) band widths and a gap (ε_G) of

$$\begin{aligned} \varepsilon_{\text{VB}} &= |t_{0,1}+t_{0,-1}| - |t_{0,1}-t_{0,-1}| - 4t_{0,2} , \\ \varepsilon_{\text{CB}} &= |t_{0,1}+t_{0,-1}| - |t_{0,1}-t_{0,-1}| + 4t_{0,2} , \\ \varepsilon_G &= 2\,|t_{0,1}-t_{0,-1}| . \end{aligned} \tag{21}$$

It is interesting to note that with this approach the gap of geometry II is estimated to be 1.28 eV, comparable with the 1.10 eV reported in Table II, suggesting that the local-density approximation does not underestimate the gap for the quasi-one-dimensional systems as much as is common for the three-dimensional systems.

In (20) it is seen that the second-nearest neighbors are not to be neglected. The hopping integrals are about 10% of those for the nearest neighbors. Furthermore, in Sec. IV we stated that the third-nearest-neighbor interactions were important in explaining the variations in the gap for *cis*-polyacetylene. Since the third-nearest-neighbor distance is about 3 Å, we can estimate the corresponding hopping integrals to be of the order of 0.3 eV.

From the first three values in (20), we estimate t_0 and α of (17) to be

$$t_0 = 3.78 \text{ eV}, \quad \alpha = 5.45 \text{ eV/Å} . \tag{22}$$

Those values are fairly different from those of Su, Schrieffer, and Heeger. From the semiempirical calculations by Grant and Batra,[30] they estimate a total π-electron bandwidth of $4t_0 = 10$ eV, giving $t_0 = 2.5$ eV. Experimental values for K (21 eV/Å^2), u_0 (0.04 Å), and ε_G (1.40 eV) are then used by SSH to obtain $\alpha = 4.1$ eV/Å.

Different parameters have been reported by Mele and Rice[48] and Baeriswyl *et al.*[49] They agree essentially with each other and are[49] $t_0 = 3$ eV, $\alpha = 6.9$ eV/Å, and $K = 50$ eV/Å.

The total energy per C_2H_2 unit can be found from (19), (15), and (18),

$$E_{\text{tot}} = E_\sigma + E_\pi \ . \qquad (23)$$

For general nearest- and second-nearest-neighbor hopping integrals a generalization of the method by Su, Schrieffer, and Heeger[47] gives

$$E_\pi = -\frac{4}{\pi}(t_{0,1}+t_{0,-1})E\left[\frac{4t_{0,1}t_{0,-1}}{(t_{0,1}+t_{0,-1})^2}\right] , \qquad (24)$$

$E(t)$ being the elliptic integral. (Note that E_π is independent of $t_{0,2}$.) Furthermore,

$$E_\sigma = 4Ku_0^2 \ . \qquad (25)$$

E_π is a decreasing function of u_0, whereas E_σ is an increasing function of u_0. The sum of the two is, with use of the parameters of SSH, found to have a minimum for $u_0 \neq 0$.

With the π-electron hopping integrals obtained in the preceding analysis, E_π changes by 0.11 eV when passing from $x = 0.5$ to $x = 0.0$, but since the total energy decreases 0.24 eV for x changing from 0.5 to 0.2 (see Table V and Fig. 6), we have to conclude that the form (25) of the σ contribution of the total energy is not correct: $E_{\text{tot}} - E_\pi$ as a function of u_0 will not give a parabola centered at $u_0 = 0$. The conclusion is not changed by including the different unit-cell lengths, i.e., by using

$$u_n = (-1)^n u_0 + C(0.5-x)^2 n \ , \qquad (26)$$

as giving the positions of the carbon atoms. The form (26) with $C \neq 0$ corresponds to the geometries we have considered better than with $C = 0$, as assumed elsewhere.

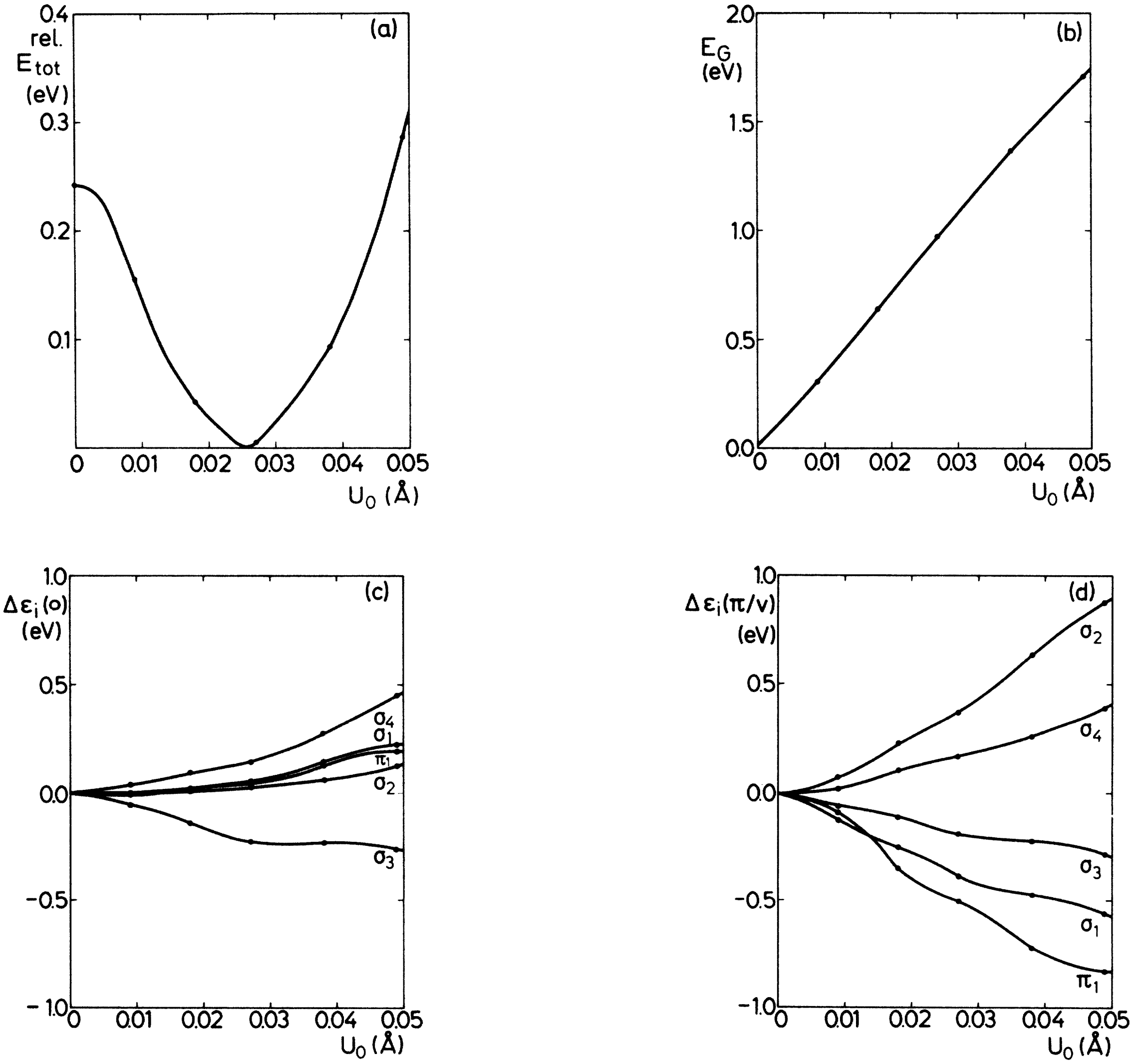

FIG. 6. Different quantities as a function of the dimerization parameter u_0: (a) relative total energy in eV per C_2H_2 unit; (b) the calculated gap in eV; (c) and (d) relative one-electron energy bands in eV at the zone center (c) and at the zone edge (d). In this figure all levels have been set to 0 for $u_0 = 0$. The optimized geometry corresponds to $u_0 = 0.025$ Å.

The total energies in Table III support this conclusion: The energy difference between dimerized and undimerized polyacetylene is larger than the 0.03 eV predicted by the SSH Hamiltonian for almost all calculations.[47]

On the other hand, we still believe that the SSH Hamiltonian can be used to describe *trans*-polyacetylene, but it has to be interpreted differently. Dimerizing *trans*-polyacetylene will, of course, increase the electron density in the shorter bonds and decrease it in the longer bonds. This effect is appropriately described by a tight-binding Hamiltonian of the form (16) [or (18) when more accuracy is needed], where the creation and annihilation operators are not restricted to π electrons any more but now create or annihilate electron densities of both σ and π types at the same time. A repulsive interaction between the atoms can, similarly, to lowest order, be written in the form (17).

This also means that the parameters for the "π" part cannot be found from values of the energy gap and the π-electron bandwidth. The parameters can only be found from the total energy, e.g., by fitting the total energies obtained in procedures similar to the present one.

That the σ electrons are also affected by the dimerization can be seen in Table V and Fig. 6, where the values of the bands at the zone center and zone edge are given. In particular, one can notice that the sum of the one-electron energies for the occupied σ bands is not constant. (The calculations reported for $x=0.50$ were not performed for x exactly equal to $\frac{1}{2}$, causing the gaps at $k=\pi/v$ seen in the Table V.) The calculations of this section and those of Sec. IV are not identical and the results differ slightly. The differences can be taken as estimates of the uncertainties of the method. In Table V we have also collected the energy gaps calculated with the parameter-free method and that obtained from (21). They differ fairly slightly.

Finally, the multipoles of the electron distribution inside the carbon atomic sphere (in those calculations the sphere radii were chosen to be 1.260 a.u. for carbon and 0.795 a.u. for hydrogen) are similar to those of Table I. The changes in $q_{C,s}$ are most likely related to the changes in the size of the unit cell. The near constancy of $q_{C,x}$ can be interpreted as being related to the near independency of the hydrogen-carbon bond on the dimerization. On the other hand, the dimerization is directly connected to the changes in $q_{C,z}$.

We will close this section by estimating some of the equilibrium parameters. We find $D_{1+x}-D_{2-x}=0.086$ Å, or $u_0=0.025$ Å. This corresponds to $x=0.23$ and to bond lengths of 1.444 and 1.358 Å, in good agreement with the experimental values [1.46 and 1.35 Å (Ref. 38), 1.44 and 1.36 Å (Ref. 50)]. The gap is then calculated to be 0.93 eV (quite underestimated compared with the experimental values of 1.4—1.8 eV) and the ionization potential to be 5.84 eV (experimental value of 4.7 eV).

VII. CONCLUSION

The present analysis of the ground state of ideal polyacetylene has split into two parts: A comparison of the electronic distribution of five fixed structures of both *trans*- and *cis*-polyacetylene, and an examination of the dimerization of the *trans* isomers.

The one-electron energy bands for the *trans* and *cis* isomers differed mainly in the position of an avoided crossing: for the σ_2 and σ_3 bands for *trans*-polyacetylene, and for the σ_3 and σ_4 bands for *cis*-polyacetylene. The electrons were well localized near the nuclei, thereby justifying making a single-polymer approximation. Not only contour plots for the electron distribution but also the multipoles of the electron densities inside the atomic spheres were useful in analyzing the bonds.

Furthermore, for *trans*-polyacetylene it was found that a dimerized geometry with lower symmetry was energetically favored when compared with the undimerized geometry with higher symmetry. In describing the dimerization of *trans*-polyacetylene, a model Hamiltonian containing a repulsive and an attractive term like that of Su, Schrieffer, and Heeger seems appropriate, but since both σ and π electrons are responsible for the dimerization, the parameters entering the model Hamiltonian can only be found from values of integrated quantities like the total energy and not from one-electron properties.

Finally, we showed that our method seems to be able to predict ground-state properties in good agreement with experimental ones.

ACKNOWLEDGMENTS

I would like to thank Andreas Bringer and Ole Krogh Andersen for a critical reading of the manuscript.

---

[1] C. K. Chiang, C. R. Fincher, Jr., Y. W. Park, A. J. Heeger, H. Shirakawa, E. J. Louis, S. C. Gau, and A. G. MacDiarmid, Phys. Rev. Lett. **39**, 1098 (1977).

[2] W. P. Su, J. R. Schrieffer, and A. J. Heeger, Phys. Rev. Lett. **42**, 1698 (1979).

[3] H. W. Streitwolf, Phys. Status Solidi B **127**, 11 (1985).

[4] D. Baeriswyl, Helv. Phys. Acta **56**, 639 (1983).

[5] M.-H. Whangbo, R. Hoffmann, and R. B. Woodward, Proc. R. Soc. London, Ser. A **366**, 23 (1979).

[6] T. Yamabe, K. Tanaka, H. Teramae, K. Fukui, A. Imamura, H. Shirakawa, and S. Ikeda, Solid State Commun. **29**, 329 (1979).

[7] T. Yamabe, K. Tanaka, H. Teramae, K. Fukui, A. Imamura, H. Shirakawa, and S. Ikeda, J. Phys. C **12**, L257 (1979).

[8] V. Young, S. H. Suck, and E. W. Hellmuth, J. Appl. Phys. **50**, 6088 (1979).

[9] V. Young, Solid State Commun. **35**, 715 (1980).

[10] M. L. Elert and C. T. White, Phys. Rev. B **28**, 7387 (1983).

[11] W. K. Ford, C. B. Duke, and A. Paton, J. Chem. Phys. **77**, 4564 (1982).

[12] R. Al-Jishi, G. A. Worrell, P. L. Taylor, M. Thakur, J. B. Lando, and A. Das, Phys. Rev. B **30**, 7281 (1984).

[13] M. Kertész, J. Koller, and A. Ažman, J. Chem. Soc. Chem. Commun. **1978**, 575 (1978).

[14] A. Karpfen and J. Petkov, Solid State Commun. **29**, 251 (1979).

[15] A. Karpfen and J. Petkov, Theor. Chim. Acta (Berlin) **53**, 65 (1979).

[16] S. Suhai, J. Chem. Phys. **73**, 3843 (1980).

[17] A. Karpfen and R. Höller, Solid State Commun. **37**, 179 (1981).

[18] J. L. Brédas, R. R. Chance, R. Silbey, G. Nicolas, and Ph. Durand, J. Chem. Phys. **75**, 255 (1981).

[19] M. Kertész, Adv. Quant. Chem. **15**, 161 (1982).

[20] J. L. Brédas, R. R. Chance, R. H. Baughman, and R. Silbey, J. Chem. Phys. **76**, 3673 (1982).

[21] B. Kirtman, W. B. Nilsson, and W. E. Palke, Solid State Commun. **46**, 791 (1983).

[22] R. Dovesi, Int. J. Quant. Chem. **26**, 197 (1984).

[23] H. Teramae, T. Yamabe, and A. Imamura, J. Chem. Phys. **81**, 3564 (1984).

[24] B. K. Rao, J. A. Darsey, and N. R. Kestner, J. Chem. Phys. **79**, 1377 (1983).

[25] B. K. Rao, J. A. Darsey, and N. R. Kestner, Phys. Rev. B **31**, 1187 (1985).

[26] Y. J. I'Haya, S. Narita, Y. Fujita, and H. Ujino, Int. J. Quant. Chem. Symp. **18**, 153 (1984).

[27] S. Suhai, Chem. Phys. Lett. **96**, 619 (1983).

[28] S. Suhai, Phys. Rev. B **27**, 3506 (1983).

[29] J. E. Falk and R. J. Fleming, J. Phys. C **8**, 627 (1975).

[30] P. M. Grant and I. P. Batra, Solid State Commun. **29**, 225 (1979).

[31] R. V. Kasowski, W. Y. Hsu, and E. B. Caruthers, J. Chem. Phys. **72**, 4896 (1980).

[32] J. W. Mintmire and C. T. White, Phys. Rev. Lett. **50**, 101 (1983).

[33] J. W. Mintmire and C. T. White, Phys. Rev. B **28**, 3283 (1983).

[34] J. von Boehm, P. Kuivalainen, and J.-L. Calais, Solid State Commun. **48**, 1085 (1983).

[35] P. M. Grant and I. P. Batra, J. Phys. (Paris) Colloq. **44**, C3-437 (1983).

[36] P. Kuivalainen, J. von Boehm, and J.-L. Calais, Mol. Cryst. Liq. Cryst. **117**, 195 (1985).

[37] M. Springborg and O. K. Andersen (unpublished).

[38] R. H. Baughman, S. L. Hsu, G. P. Pez, and A. J. Signorelli, J. Chem. Phys. **68**, 5405 (1978).

[39] L. Pauling, *The Nature of the Chemical Bond,* 3rd ed. (Cornell University Press, Ithaca, 1960), pp. 234–236.

[40] C.-O. Almbladh and U. von Barth, Phys. Rev. B **31**, 3231 (1985).

[41] S. Roth (private communication).

[42] V. Bonifacic and S. Huzinaga, J. Chem. Phys. **60**, 2779 (1974).

[43] C. Møller and M. S. Plesset, Phys. Rev. **46**, 618 (1934).

[44] We have performed calculations with similar approximations and obtained qualitatively the same results as those of Falk and Fleming, Ref. 29.

[45] C. R. Fincher, Jr., C.-E. Chen, A. J. Heeger, A. G. MacDiarmid, and J. B. Hastings, Phys. Rev. Lett. **48**, 100 (1982).

[46] C. R. Fincer, Jr., M. Ozaki, M. Tanaka, D. Peebles, L. Lauchlan, A. J. Heeger, and A. G. MacDiarmid, Phys. Rev. B **20**, 1589 (1979).

[47] W. P. Su, J. R. Schrieffer, and A. J. Heeger, Phys. Rev. B **22**, 2099 (1980); **28**, 1138(E) (1983).

[48] E. J. Mele and M. J. Rice, Phys. Rev. Lett. **45**, 926 (1980).

[49] D. Baeriswyl, G. Harbeke, H. Kiess, and W. Meyer, in *Electronic Properties of Polymers,* edited by J. Mort and G. Pfister (Wiley, New York, 1982).

[50] C. S. Yannoni and T. C. Clarke, Phys. Rev. Lett. **51**, 1191 (1983).